Journal of Catalysis **195,** 38–45 (2000)
doi:10.1006/jcat.2000.2982, available online at http://www.idealibrary.com on IDEAL®

Simultaneous Determination of Reaction Kinetics and Oxygen Activity in an Oxidic Multicomponent Catalyst during Partial Oxidations

M. Estenfelder[1] and H.-G. Lintz[2]

Institut für Chemische Verfahrenstechnik, Universität Karlsruhe (TH), 76128 Karlsruhe, Germany

Received February 24, 2000; revised May 18, 2000; accepted June 27, 2000

The partial oxidation of an aldehyde to a carboxylic acid has been studied over an oxidic multicomponent catalyst, mainly based on Mo, V, and Cu. The experimental setup enabled the simultaneous determination of reaction kinetics and the oxygen activity of the catalyst under working conditions. The kinetic measurements were performed by monitoring the gas phase composition along the length of a fixed bed of catalyst. The reactor was treated as an isothermal plug flow system. The reaction kinetics can be described by a simple triangular network consisting of the main reaction (aldehyde to carboxylic acid), a consecutive reaction (carboxylic acid to by-products), and a parallel reaction (aldehyde to by-products). The simultaneous determination of the oxygen activity in the catalyst has been realized by use of a solid electrolyte potentiometry (SEP) cell, connected to the apparatus. The cell consists of an oxygen-ion-conducting solid electrolyte ($ZrO_2 + 8.5$ wt% Y_2O_3) coated with a platinum reference electrode on one side and with the catalytically active electrode on the other side, the latter being made of the same catalyst material used in the tubular reactor. While the measuring electrode was in contact with the gas phase to be analyzed, the reference electrode was always flushed with air. The oxygen activity of the catalyst is derived from the measured potential difference between both electrodes. The results clearly show that the catalyst under working conditions is always in a reduced state rather than in equilibrium with the oxygen in the surrounding gas phase. The axial profile of the oxygen activity along the fixed bed reactor indicates the existence of two different oxidation states of the catalyst. The more reduced state in the first part of the reactor reflects the strong interaction of the aldehyde with the catalyst; the less reduced one in the final part of the reactor indicates the weaker interaction of the catalyst with the intermediate carboxylic acid. Both the kinetic and potentiometric measurements lead to consistent results. © 2000 Academic Press

Key Words: **solid electrolyte potentiometry; oxygen activity; oxidation reaction; oxygen transfer; kinetic,** *in situ*; **multicomponent oxides.**

1. INTRODUCTION

Multicomponent oxidic catalysts are commonly used in the partial oxidation of hydrocarbons and other organic compounds. They may show—at reasonably high activity—extremely good selectivities for the products aimed at (1). The efficiency of such catalysts and the synergy effects observed in the presence of one or more well-defined oxidic phases raise the question of their origin. Different explanations of these synergetic effects, the enhancement of both activity and selectivity, have been proposed (2). They cover the change of morphology of the catalyst under the conditions of the catalytic reaction (3), the remote control process (4), which is due to spillover of oxygen from one oxide to another, and the interactions between phases (5).

Anyhow, the availability and transfer of oxygen is a function of the phase composition of the catalyst, its oxidation state. Under operating conditions this oxidation state is not only determined by the oxygen partial pressure in the gas phase but also results from the rates of oxygen transfer to and from the solid. There is a mutual interaction of the gas phase and the catalyzing solid. One may wonder how the latter is modified when the composition of the gas phase is totally changed from the feed to the product stream. One may even suspect that the use of multicomponent catalysts, often not justified by any topographic reason, is determined by the necessity to "buffer" the oxidation state independent of the gas phase composition.

To characterize the oxidation state of a solid, Carl Wagner (6) proposed the measurement of its oxygen activity by a potentiometric method. It is based on the use of an ion-conducting solid as the electrolyte. Two porous electrodes of a galvanic cell are separated gas-tight by the solid electrolyte. One electrode is exposed to the reacting gas mixture and acts simultaneously as the catalyst; the second electrode is in contact with a given value of the oxygen partial pressure as reference. The measurement of the potential difference between these two electrodes leads to the value of the oxygen activity in the catalyst, which is operationally defined by this method, named solid electrolyte potentiometry (SEP).

[1] Now with Consortium für elektrochemische Industrie, Zielstattstraße 20, 81379 München, Germany.

[2] To whom correspondence should be addressed. Institut für Chemische Verfahrenstechnik, Universität Karlsruhe (TH), Kaiserstraße 12, Gebäude 30.44, 76128 Karlsruhe. Fax: +49-(0)721-608-6118. E-mail: Cvt@ciw.uni-karlsruhe.de.

0021-9517/00 $35.00

In the following we present an experimental setup that allows the simultaneous determination of the gas phase composition and the oxygen activity of the solid catalyst under operating conditions along a tubular fixed bed reactor. Preliminary results of the partial oxidation of acrolein to acrylic acid on an oxidic catalyst illustrate the possibilities of the experimental approach.

2. METHODS

The experimental setup (Fig. 1) can be divided into two parts, the fixed bed reactor used for the kinetic measurements and a second device intended for the solid electrolyte potentiometry.

2.1. Kinetic Measurements

The fixed bed reactor has been described in detail elsewhere (1, 7). The reaction mixture is admitted through thermal mass flow controllers, the concentrations of acrolein and water being fixed by loading a stream of nitrogen or air via two saturation–condensation systems operated at constant pressure and temperature. The kinetic experiments were carried out in a tubular reactor (1500-mm length, 15-mm internal diameter) at a pressure of 1.4 bar and a temperature of 300°C. A fixed bed consisting of 200 g of spherical egg-shell catalyst was employed. The feed stream contained 2–4 mol% acrolein, 3–11 mol% oxygen, 0–5 mol% water, and balance nitrogen at volume flow rates of 60 or 80 ml/s (NTP).

The reactor was divided into nine segments with separate electrical heating and individual temperature control to maintain isothermal operation. Heated capillaries were located at the inlet and at the outlet of each segment leading to the analytical section. Thus, the gas phase composition along the length of the fixed bed could be monitored by distributed local sampling. In contrast to the setup used before (1, 7) each side stream selected by use of a multiposition valve entered a SEP cell (cf. 2.2) prior to analysis by gas chromatography (organic components), infrared photometers (CO, CO_2), and a magnetomechanic device (O_2).

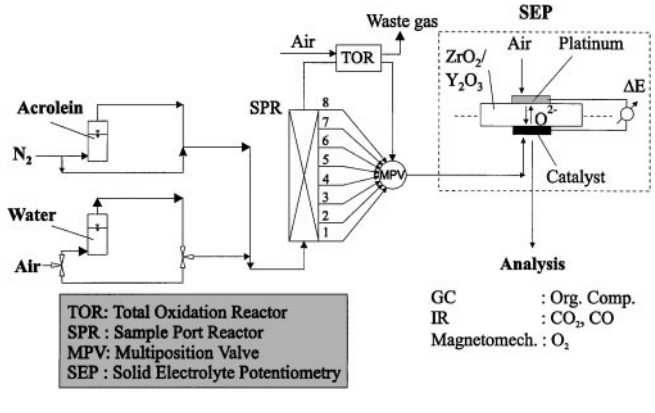

FIG. 1. Schematic diagram of the experimental setup.

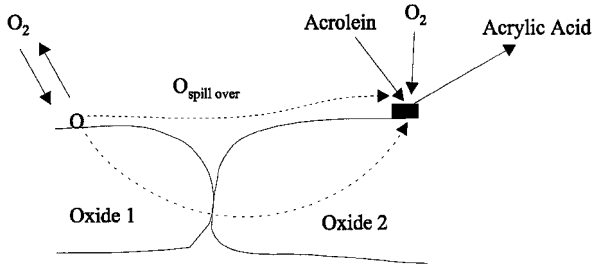

FIG. 2. Oxygen transfer in a mixture of two oxides.

2.2. Potentiometric Measurements

The principles of the SEP measurements have been described in detail elsewhere (8). The underlying assumptions for its use in the case of single phase, oxidic catalysts have been equally discussed (9). As long as the solid is in equilibrium with the surrounding gas phase, the value of its oxygen activity is determined by the oxygen partial pressure:

$$a_O^2 \equiv p_{O_2}. \qquad [1]$$

As soon as there is an oxygen sink, the oxygen activity is generally less than the oxygen partial pressure ($a_O^2 < p_{O_2}$) but can still be measured by SEP.

However, applying SEP to a multicomponent catalyst, as it is done in this study, accounts for further assumptions. Therefore, let us discuss the meaning of the oxygen activity in the mixture of two oxidic phases, oxide 1 and oxide 2. We assume that the oxygen activity in the pure oxide 1 under the same reaction conditions is higher than that in oxide 2, always considering a constant value of the oxygen activity throughout the pure oxides:

$$a^2_{O,\text{oxide 1}} > a^2_{O,\text{oxide 2}}. \qquad [2]$$

Furthermore, we assume that both oxides exist side by side separately in the mixture and do not form a new oxidic phase. If the reactant mixture (acrolein, oxygen, water, acrylic acid) is applied, an oxygen transfer between both oxidic phases due to the gradient in the oxygen activity will occur. As the oxygen activity in the pure oxide 1 is supposed to be higher than that in the pure oxide 2 under the same conditions, the former will serve as an oxygen donor and the latter as an oxygen acceptor. Oxygen is transmitted in the solid from oxide 1 to oxide 2 via a spillover mechanism along the catalyst surface (cf. Fig. 2) or via bulk, both mechanisms leading to a reoxidation of oxide 2. Thus, SEP provides a possibility of confirming the ranking of the strength of solid oxygen acceptors and donors suggested by Delmon and Weng (4) and discussed elsewhere (10). Following the above-mentioned concept, strong solid oxygen

acceptors should correspond to low values of oxygen activity and strong oxygen donors to high values when exposed to the same reactant mixture.

SEP was carried out in a galvanic cell consisting of a solid electrolyte disk (thickness 2 mm) made of yttria (8.5 wt%) stabilized zirconia, coated with the same active component (cf. 2.3) used in the reactor on the measuring side and with a porous platinum electrode on the reference side. The measuring electrode was in contact with the gas phase to be analysed and simultaneously worked as a catalyst. The reference electrode was flushed with air. Both electrodes were connected via a high ohmic volt meter. Temperature and pressure in the cell were the same as those in the fixed bed reactor ($T = 300°C$, $p = 1.4$ bar). The possibilities to apply SEP at such temperatures have been discussed in detail elsewhere (11).

It is the aim of the potentiometric measurements to determine the distribution of oxygen activity in the catalyst along the fixed bed in parallel to the concentration profile in the gas phase. To avoid the use of one galvanic cell at each sampling port, the side streams collected sequentially passed over the catalyst electrode of the SEP cell shown in Fig. 1.

The catalyst electrode has been prepared in a way that the additional acrolein conversion in the cell was kept below 10% in any case. Thus, we can safely assume a constant gas phase composition in the SEP cell and the measured potential difference between the electrodes is characteristic for the oxidation state of the catalyst under the reaction conditions and the gas phase composition at the corresponding sample port of the tubular reactor. In addition, there are no inner transport resistances due to the small film thickness ($<50\ \mu$m) of the catalyst electrode.

2.3. Catalyst and Electrode Preparation

The fixed bed contained 200 g of spherical egg-shell catalysts, diluted by shattered steatite particles ($0.9 < d < 1.6$ mm) in a mass ratio 1:1 to ascertain plug flow. The egg-shell catalyst used throughout the study was prepared by coating spherical steatite particles of 4- to 5-mm diameter with a porous oxidic layer. The final catalyst contained 10 wt% active compound, the thickness of the shell being 100 μm. The oxidic catalyst consisted mainly of Mo, V, and Cu; its preparation has been described elsewhere (12). The overall stoichiometry of the multicomponent oxide with respect to its main constituents is $Mo_{12}V_3Cu_{2.2}O_{44}$.

The reference electrode was prepared by coating the electrolyte with a thin layer (80 μm) of a commercial platinum paste and sintering the film for 2 h at a temperature of 800°C.

The measuring electrode employed the same catalyst powder (12) that was used to prepare the egg-shell catalyst. It was mixed with an organic binder, giving a viscous paste. The solid electrolyte was coated with this paste up to a film thickness of 80 μm and sintered for 1 h at 320°C, leading to a sufficient adherence of the porous electrode on the electrolyte.

2.4. Data Evaluation

2.4.1. Kinetic measurements. By using the experimental setup shown in Fig. 1, we measured concentration profiles as a function of the modified residence time t_m, which is defined by the ratio of the mass of the catalytically active oxide $m_{C,z}$ between the reactor inlet and sample port z and the volume flow $\dot{V}$ through the reactor:

$$t_{m,z} = \frac{m_{C,z}}{\dot{V}}. \qquad [3]$$

As the volume flow is constant throughout the reactor, we can define

—the acrolein conversion X_z up to sampling port z:

$$X_z = \frac{c_{\text{Acrolein,in}} - c_{\text{Acrolein},z}}{c_{\text{Acrolein,in}}}, \qquad [4]$$

—the integral reactor selectivity ${}^{R}S_{i,z}$ for the formation of product i at port z:

$${}^{R}S_{i,z} = \frac{c_{i,z} \cdot \varepsilon_i}{(c_{\text{Acrolein,in}} - c_{\text{Acrolein},z}) \cdot \varepsilon_{\text{Acrolein}}}. \qquad [5]$$

By using the dimensionless factor ε_i, which designates the number of carbon atoms in one molecule of species i, the reactor selectivity is normalized to values between 0 and 1.

It has been shown earlier that the kinetics of selective acrolein oxidation can be described by using a simple network (cf. Fig. 3) of chemical reactions (7). CO_2, CO, and acetic acid generated in small amounts can be lumped together into one pseudospecies ("by-products"). The network consists of the main reaction from acrolein to acrylic acid, a parallel reaction of acrolein to by-products and the consecutive reaction of acrylic acid to by-products.

The rate of the individual reactions in this system can be represented by the rate equations listed above where the reaction rate in pathway i, j, $r_{mi,j}$ is given in mol $g^{-1}\,s^{-1}$. All rate coefficients $k_{mi,j}$ are related to the mass of the catalytically active compound. Mass balancing the reactor in steady state leads to a set of three simultaneous differential

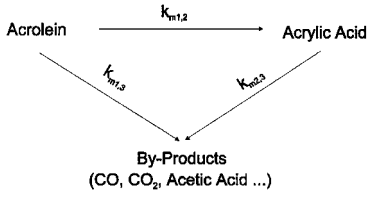

$$r_{m1,2} = \frac{k_{m1,2} \cdot c_{\text{Acrolein}}}{1 + b \cdot c_{\text{Acrolein}}} \qquad [6]$$

$$r_{m1,3} = \frac{k_{m1,3} \cdot c_{\text{Acrolein}}}{1 + b \cdot c_{\text{Acrolein}}} \qquad [7]$$

$$r_{m2,3} = k_{m2,3} \cdot c_{\text{Acrylic Acid}} \qquad [8]$$

FIG. 3. Network of acrolein oxidation and rate equations.

equations that can be solved numerically by use of the Runge–Kutta method. The values of the kinetic coefficients $k_{mi,j}$ and b are determined by curve fitting of the calculated concentration profiles to the experimentally determined ones.

We can derive characteristic parameters for the activity and selectivity of the used catalyst from these coefficients:

—Due to the fractional order of the parallel reactions $r_{m1,2}$ and $r_{m1,3}$, we make use of a conversion-dependent parameter, k^*_{m1}, characterizing the activity of the catalyst with respect to acrolein conversion:

$$k^*_{m1} = \frac{k_{m1,2} + k_{m1,3}}{1 - \frac{b \cdot X^*}{\ln(1 - X^*)}} = k^*_{m1,2} + k^*_{m1,3}. \quad [9]$$

k^*_{m1} may be considered as the pseudo-first-order rate coefficient, giving the same acrolein conversion X^* at the same residence time t_m at the reactor outlet. Its derivation has been described elsewhere (13). k^*_{m1} is calculated for $X^* = 0.99$, as the maximum yield of acrylic acid is always obtained at conversions near that value.

—For a given catalyst and temperature the course of selectivity with respect to the production of the intermediate acrylic acid as a function of conversion is fixed by two parameters, the grain selectivity toward acrylic acid ${}^{K}S_{\text{Acrylic Acid}}$,

$${}^{K}S_{\text{Acrylic Acid}} \equiv \lim_{X_{\text{Acrolein}} \to 0} {}^{R}S_{\text{Acrylic Acid}} = \frac{k_{m1,2}}{k_{m1,2} + k_{m1,3}}, \quad [10]$$

and the grain stability of the metastable intermediate acrylic acid:

$${}^{K}\lambda_{\text{Acrylic Acid}} = \frac{k^*_{m1,2}}{k_{m2,3}}. \quad [11]$$

Both quantities have been introduced and discussed by Riekert (14) in the case of a similar triangular reaction network.

2.4.2. Potentiometric measurements. As stated above, the oxygen activity a^2_O in the catalyst is operationally defined by the potentiometric measurement. Its value is related to the experimentally determined potential difference ΔE (open circuit potential) via the NERNST equation

$$\Delta E = \frac{R \cdot T}{4 \cdot F} \cdot \ln \frac{a^2_O}{p_{O_2,\text{Ref}}}, \quad [12]$$

where $p_{O_2,\text{Ref}}$ designates the oxygen partial pressure at the reference side and F is the Faraday constant ($F = 96486$ C mol^{-1}). The relation is based on the potential-determining reaction that takes place at the three-phase boundary line gas–electrode–electrolyte at both electrodes.

$$O_{2,g} + 4e^-_{(\text{Electrode})} \leftrightarrow 2O^{2-}_{(\text{Electrode})}. \quad [R1]$$

As mentioned before, the oxygen activity in the solid is equal to the oxygen partial pressure in the gas phase if the oxygen in the gas phase is in equilibrium with the oxygen in the solid catalyst ($a^2_O \equiv p_{O_2}$, cf. Eq. [1]).

Equation [1] is always valid if the gas phase over the catalyst electrode only consists of oxygen and inert components (for example, nitrogen). Additionally, Eq. [1] also holds under reaction conditions if the time constant of the oxygen uptake of the catalyst from the gas phase is much smaller than the time constant of the oxygen removal from the catalyst by a gaseous oxygen acceptor A (for example, $A =$ acrolein, acrylic acid). We call this case *slow reaction*.

For the discussion of the potentiometric measurements, we need the rate of total oxygen consumption at the catalyst $r^-_{m,O_2,\text{total}}$, which under the conditions investigated can be obtained under consideration of the reaction stoichiometry of the reaction paths (15) shown in Fig. 3 as follows:

$$r^-_{m,O_2,\text{total}} = 0.5 \cdot r_{m1,2} + 2.8 \cdot r_{m1,3} + 2.2 \cdot r_{m2,3}. \quad [13]$$

Following Eq. [13], only the oxidation reactions of acrolein and acrylic acid contribute to the value of $r^-_{m,O_2,\text{total}}$. Other oxidation reactions of other gaseous oxygen acceptors can be neglected either due to the very low concentrations of the gaseous oxygen acceptor (acetic acid, acetaldehyde, aceton) or for kinetic reasons (CO) since the rate of CO oxidation has been found to be several orders of magnitude lower than the rate of acrolein or acrylic acid oxidation (16).

3. RESULTS

3.1. Typical Concentration and Oxygen Activity Profiles

Typical results of the combined kinetic and potentiometric measurements are shown in Fig. 4. The experimentally determined concentration profiles in the gas phase (left axis) and the oxygen activity of the catalyst (right axis) are plotted against the modified residence time t_m. The solid lines are the results of the kinetic model calculations, obtained by the procedure described in the preceding paragraph. The agreement of the simulation with the experimental measurements justifies the description by a simplified network.

Table 1 summarizes the values of the main parameters determined as described in section 2.4.1. It is interesting to note that the value of $k_{m1,3}$, obtained after curve fitting, is equal to 0 at the temperature considered ($T = 300^\circ$C). This means that the main reaction of acrolein to acrylic acid is much faster than the parallel reaction of acrolein to byproducts. Furthermore, the rate of oxidation of acrolein to acrylic acid is about 2 orders of magnitude higher than the rate of the consecutive oxidation of acrylic acid as reflected by the values of k^*_{m1} and $k_{m2,3}$. The low rate of acrylic acid oxidation in combination with a high rate of acrylic acid production by acrolein oxidation leads to a high value of

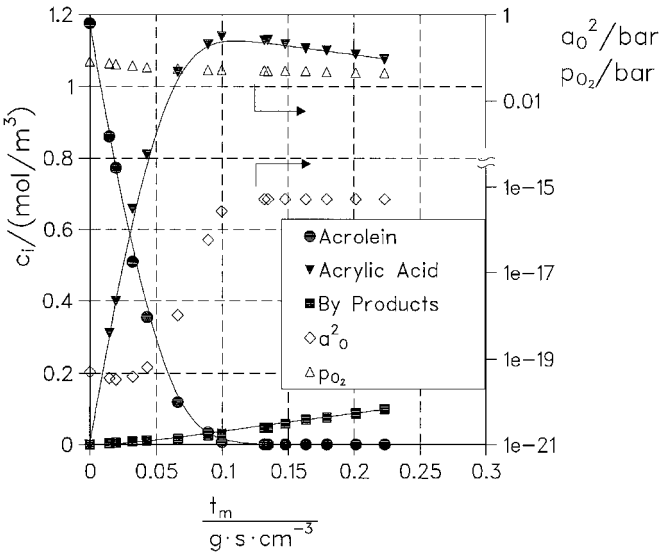

FIG. 4. Product distribution (left axis), oxygen activity, and oxygen partial pressure (right axis) as a function of the modified residence time, $x_{O_2,in} = 5.8\%$, $x_{Acrolein,in} = 4\%$, $x_{H_2O,in} = 5\%$, and $T = 300°C$. Symbols, experimental data; lines, calculated after curve fitting.

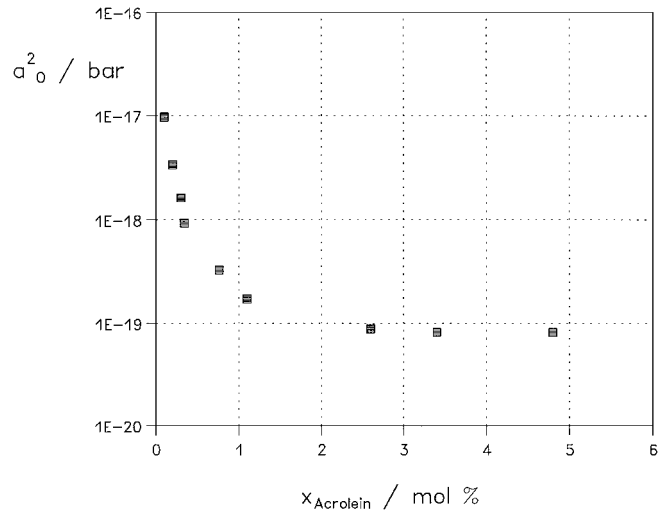

FIG. 5. The oxygen activity as a function of the molar fraction of acrolein, $T = 300°C$, $x_{O_2,in} = 5.8\%$, and $x_{H_2O,in} = 5\%$.

the stability parameter $^{int}\lambda$, which is one major reason for the high acrylic acid yield $Y_{Acrylic\ Acid}$ of 95%.

Let us now consider the evolution of the oxygen activity of the catalyst along the fixed bed reactor. No discontinuity could be observed but a continuous profile was obtained. From the reactor entrance the values of a_O^2 remain at a constant, low level, nearly independent of the composition of the gas phase over a wide range of acrolein conversion ($X = 75\%$). This is surprising since the molar fraction of acrolein decreases from 4% at the reactor inlet to 1%. For acrolein conversion near 100%, the oxygen activity strongly increases, reaching a second constant level at complete acrolein conversion. (Here, complete acrolein conversion means that acrolein is no longer detectable in the gas phase by gas chromatography.)

The values of the oxygen activity are always at least 12 orders of magnitude lower than the oxygen partial pressure (open triangles) of the corresponding gas phase over the catalyst. This clearly indicates a partially reduced state of the catalyst rather than an equilibrium between the oxygen in the catalyst and the surrounding gas phase since in the latter case the oxygen activity should equal the oxygen partial pressure (cf. Eq. [1]).

For further validation of the congruence of kinetic and potentiometric measurements, we determined the influence of acrolein concentration on the oxygen activity in the catalyst by increasing it step by step at constant values of oxygen and water concentrations. The results shown in Fig. 5 illustrate that an increase of the acrolein molar fraction from 2% to 5% only leads to a small change in the oxygen activity in the catalyst, indicating the existence of a lower limit of the oxygen activity at high acrolein concentrations. The kinetic experiments show the same saturation effect at high acrolein concentration through the fractional orders of the formal rate expressions derived for the acrolein consumption (reaction paths 1,2 and 1,3). Thus, the consistency of the kinetic and potentiometric measurements is once more illustrated.

TABLE 1

Kinetic and Characteristic Parameters at 300°C: $x_{O_2,in} = 5.8\%$; $x_{Acrolein,in} = 4\%$; $x_{H_2O,in} = 5\%$

Kinetic parameters				Characteristic parameters			
$k_{m1,2}$[a]	$k_{m1,3}$	$k_{m2,3}$	b	$Y^{max}_{Acrylic\ Acid}$	$^{K}S_{Acrylic\ Acid}$	$^{int}\lambda_{Acrylic\ Acid}$	k^*_{ml}
70	0	0.43	3.5	0.95	1	93	40

[a] The values of $k_{mi,j}$ and k^*_{m1} are always given in cm^3/(g s).

3.2. The Correlation between Oxygen Activity, Oxygen Partial Pressure, and the Total Rate of Oxygen Consumption at the Catalyst

For a detailed understanding of the oxygen activity profile along the tubular reactor, we first have to discuss the main parameters influencing its value. Let us first consider the case of an oxygen acceptor, A, in the gas phase, which is oxidized to AO at constant temperature and pressure:

$$A + 0.5O_2 \rightarrow AO. \qquad [R2]$$

We may separate the global reaction into two elementary steps, the oxygen uptake by the solid catalyst and the consumption of this oxygen by reaction with the gaseous acceptor A, a concept first proposed by Wagner and Hauffe (17) and Mars and van Krevelen (18). We may further expect that, at constant gas phase composition ($p_{O_2,1} = const.$,

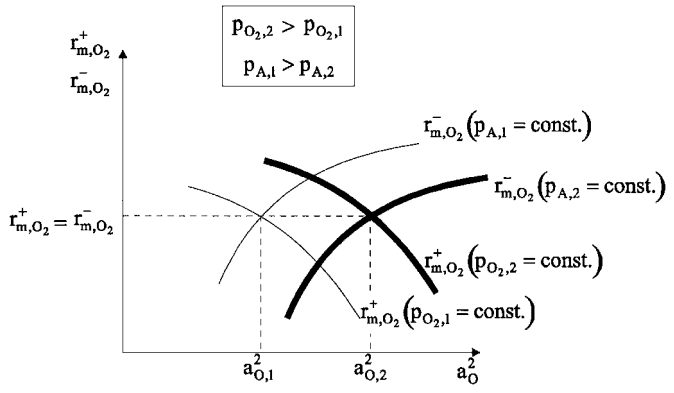

FIG. 6. Rates of oxygen consumption and oxygen uptake as a function of the oxygen activity and gas phase composition.

$p_{A,1} = \text{const.}$), the rate of oxygen uptake on the catalyst r^+_{m,O_2} decreases with rising oxygen activity in the catalyst, whereas the rate of oxygen consumption r^-_{m,O_2} on the catalyst due to the oxidation of the gaseous acceptor A to AO increases (thin lines in Fig. 6). Under steady state conditions both rates are equal and determine a stationary value of the oxygen activity $a^2_{O,1}$.

On the other hand, we may assume a positive reaction order of r^+_{m,O_2} with respect to p_{O_2} and of r^-_{m,O_2} with respect to p_A. Therefore, we can imagine a second mixture with $p_{O_2,2} > p_{O_2,1}$ and $p_{A,2} < p_{A,1}$ (fat lines in Fig. 6), which results in the same value of the reaction rate as that in the first case but in a higher oxygen activity of the catalyst, $a^2_{O,2}$.

In conclusion, the stationary value of the oxygen activity of a solid catalyst in contact with a reactive gas phase is not determined by the mere oxidation rate but depends on two parameters, e.g., the oxygen partial pressure p_{O_2} and the oxygen consumption rate r^-_{m,O_2} and we can write:

$$a^2_O = f\left(p_{O_2}, r^-_{m,O_2}\right). \qquad [14]$$

Both parameters vary along the tubular reactor.

At this point the question arises of how we have to enlarge these considerations if several oxygen transfer reactions are catalyzed by the same oxide as that in the oxidation of acrolein and acrylic acid in the present study. Brück (19) has shown in the case of catalytic reduction of nitrogen oxides over V_2O_5/TiO_2 catalysts that at constant oxygen partial pressure the oxygen activity in the catalyst is correlated to the global oxygen consumption rate $r^-_{m,O_2,total}$, which is calculated from the sum of the rates in the different oxygen-consuming steps. We may therefore suppose that in the present study the oxygen activity is a function of the oxygen partial pressure and the *total* rate of oxygen consumption $r^-_{m,O_2,total}$ in accordance with Eqs. [13] and [14] is replaced by

$$a^2_O = f\left(p_{O_2}, r^-_{m,O_2,total}\right). \qquad [15]$$

The mathematical form of the relationship between oxygen activity, oxygen partial pressure, and total rate of oxygen consumption is not predictable a priori as the values of $r^-_{m,O_2,total}$ and p_{O_2} change over the length of the tubular reactor. The total rate of oxygen consumption $r^-_{m,O_2,total}$ decreases with rising residence time in the reactor due to the decrease of the acrolein concentration, which should lead to higher oxygen activity. On the other hand, the oxygen concentration in the gas phase is simultaneously reduced, which in contrast should lower the oxygen activity. The tendency of the oxygen activity to rise with increasing oxygen concentration and decreasing total rate of oxygen consumption may be described in a general form by Eq. [16]:

$$a^2_O = f\left\{\frac{p_{O_2}}{r^-_{m,O_2,total}}\right\}. \qquad [16]$$

The parallel evolution of a^2_O and $p_{O_2}/r^-_{m,O_2,total}$ as a function of acrolein conversion is represented in Fig. 7. The result clearly indicates that a correlation between both quantities should indeed exist. We can specify this correlation by plotting the oxygen activity a^2_O against $p_{O_2}/r^-_{m,O_2,total}$ in a double logarithmic scale (cf. Fig. 8). The symbols in Fig. 8 represent experimental data from seven series of measurements with different feed compositions. We obtain a straight line with a slope of 4. Thus, we can derive an unambiguous correlation between the oxygen activity a^2_O and $p_{O_2}/r^-_{m,O_2,total}$ at the considered temperature (300°C):

$$a^2_O = f\left\{\left(\frac{p_{O_2}}{r^-_{m,O_2,total}}\right)^4\right\}. \qquad [17]$$

This correlation describes the oxidation state of the catalyst to be expected under working conditions.

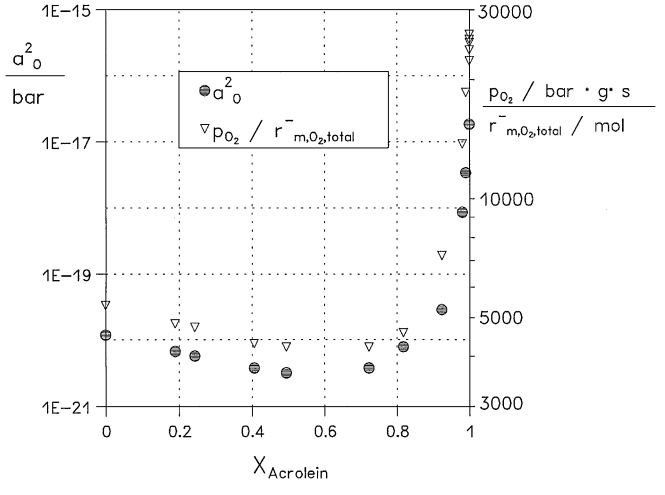

FIG. 7. Oxygen activity and $p_{O_2}/r^-_{m,O_2,total}$ as a function of acrolein conversion at 300°C, $x_{O_2,in} = 3\%$, $x_{Acrolein,in} = 4\%$, and $x_{H_2O,in} = 5\%$.

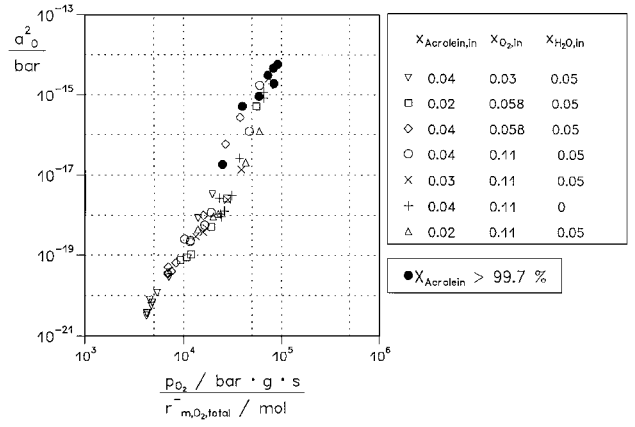

FIG. 8. Oxygen activity as a function of $p_{O_2}/r^-_{m,O_2,total}$ at different feed gas compositions.

3.3. Interpretation of the Oxygen Activity Profile along the Integral Reactor

Keeping in mind Eq. [17], we can now easily explain the form of the oxygen activity profile along the reactor as shown typically in Figs. 4 and 7. Considering that the total rate of oxygen consumption $r^-_{m,O_2,total}$ is composed of the oxidation rates of acrolein (reaction paths 1,2 and 1,3) and of acrylic acid oxidation (reaction path 2,3, cf. Eq. [6], we may divide the reactor into three different regions of acrolein conversion:

(a) region 1: $X_{Acrolein} < 70\%$.
(Depending on the feed composition, we determined values of acrolein conversion between 70% and 90% as the limit of region 1.)
As long as the acrolein conversion is lower than 70%, $r^-_{m,O_2,total}$ mainly depends on the rate of acrolein oxidation and the contribution of the consecutive reaction (path 2, 3) to the value of $r^-_{m,O_2,total}$ is negligible. Indeed, the value of the kinetic parameter $k_{m2,3}$ is about 2 orders of magnitude lower than k^*_{ml} (cf. Table 1), the latter reflecting the contribution of acrolein oxidation to $r^-_{m,O_2,total}$. In this region the values of $p_{O_2}/r^-_{m,O_2,total}$ and as a consequence the oxygen activity a^2_O remain on a more or less constant low level (cf. Fig. 7). The absolute values of the oxygen activity ($10^{-21} < a^2_O < 10^{-17}$ bar) depend on the feed composition. They constitute the lower part in Fig. 8.

(b) region 2: $70\% < X_{Acrolein} < 99.7\%$.
When the acrolein conversion lies inbetween 70% and 99.7%, the rates of acrolein oxidation and acrylic acid further oxidation are of the same order due to low acrolein and high acrylic acid concentrations. In this region the oxygen activity strongly rises with increasing conversion (cf. Figs. 4 and 7). These values of oxygen activity ($a^2_O > 10^{-17}$ bar) constitute the upper part in Fig. 8.

(c) region 3: $X_{Acrolein} > 99.7\%$.
When acrolein is no longer detectable in the gas phase ($X_{Acrolein} > 99.7\%$)—in a technical scale we would say acrolein is completely converted—the course of the oxygen activity along the tubular reactor again reaches a constant level (cf. Fig. 4). The oxygen activity in this region only depends on the concentrations of oxygen and acrylic acid, which determine the total oxygen consumption rate $r^-_{m,O_2,total}$. For acrolein conversions >99.7% the concentrations of both acrylic acid and oxygen decrease with increasing residence time in the reactor, leading to a higher oxygen activity in the case of acrylic acid and to a lower oxygen activity in the case of oxygen. This compensation effect in combination with very small relative changes of acrylic acid and oxygen concentration are the reasons for the constant oxygen activity in the region of complete acrolein conversion as shown in Fig. 4.

As an additional conclusion, for a given feed composition every series of measurements results in only one characteristic couple (a^2_O, $p_{O_2}/r^-_{m,O_2,total}$) in the region of complete acrolein conversion, each represented by one closed circle in Fig. 8.

It is interesting to note that the correlation between the oxygen activity and $p_{O_2}/r^-_{m,O_2,total}$ can be described by the same straight line, even in the region of complete acrolein conversion. This is a strong hint that, as supposed in section 3.2, the total rate of oxygen consumption is indeed responsible for the oxygen activity in the catalyst, independent of the individual rates of acrolein and acrylic acid oxidation.

4. DISCUSSION

In the present study gas phase composition and the oxidation state of the catalyst, represented by its oxygen activity, were both monitored by simultaneous kinetic and potentiometric measurements in the case of selective oxidation of acrolein. To our knowledge, it is the first time that the oxygen activity profile along an integrally operated tubular reactor could be determined by use of solid electrolyte potentiometry in such a partial oxidation over an oxidic multicomponent catalyst.

The SEP measurements have been made in the stationary state. Due to the low conversion in the cell ($X_{SEP} < 10\%$), the solid catalyst as a whole is in contact with a gas mixture of identical composition, independent of its local position. Additionally, as already mentioned, we can also rule out concentration profiles in the solid as a consequence of mass transport limitation. Therefore, there should be no global gradient in the oxygen activity in the solid if steady state is attained. Consequently, there is no net diffusion of oxygen through the solid to the three-phase boundary gas–catalyst electrode–solid electrolyte. It follows that the oxygen activity determined is representative of the whole catalyst under working conditions.

However, this does not exclude the existence of differences in composition and/or structure on a microscopic scale. The coexistence of two phases as a patchwork in the catalyst ("Mosaik-Struktur") has first been discussed by Wagner (20). That structure implies that constant fluxes

of material between the gas phase and the solid are accompanied by the diffusion of species on a microscopic scale due to local activity gradients, e.g., of the oxygen activity. In such cases the determined value of the oxygen activity represents a mean value characteristic of the actual structure of the catalyst. If it remains constant, we may expect that neither the macroscopic nor the microscopic state of the solid has changed as it is highly improbable that structural/compositional variations of the catalyst are compensated in such a way that the resulting value of a_O^2 remains constant.

Thus, even if we cannot use SEP to discriminate locally between domains of different structures/compositions, we can use the measured oxygen activity to operationally define an "oxidation state" of the catalyst under working conditions. As in the case of one stoichiometrically defined oxide (21), it results from the rates of oxygen transfer to and from the solid. The lower the value of the oxygen activity obtained by the measurement, the more reduced the catalyst by comparison to a former value.

The results show that in the case of acrolein partial oxidation two domains of a nearly constant oxygen activity in the solid exist. This indicates that two values of the oxidation state of the catalyst are buffered in the system under consideration in spite of dramatic variations of the composition of the oxygen acceptors acrolein and acrylic acid in the gas phase.

When we compare the values of the kinetic coefficients ($k^*_{m1,2} = 40$ cm^3/(g s) and $k_{m2,3} = 0.43$ cm^3/(g s) in the case of Fig. 4), it becomes obvious that the rate of acrolein oxidation to acrylic acid (reaction path 1,2 in Fig. 3) is about 2 orders of magnitude higher than the rate of acrylic acid oxidation to by-products (cf. reaction path 2,3 in Fig. 3). In accordance with this, we obtain extremely low values of the oxygen activity in the catalyst in a gas phase containing acrolein and values several orders of magnitude higher if the mixture contains acrylic acid instead (cf. Figs. 4 and 7). This shows the strong interaction of acrolein and the weaker interaction of acrylic acid with the catalyst. Acrolein, by reacting to acrylic acid, is able to efficiently remove oxygen from the catalyst whereas acrylic acid, once formed, is rather stable, only a small fraction being further oxidized to by-products. Thus, acrolein acts as a stronger reducing agent than the product acrylic acid, which is in accordance with the high value of the stability parameter ${}^K\lambda_{\text{Acrylic Acid}}$ for the latter, derived through the kinetic measurements.

In conclusion, we can say that a good catalyst for the production of acrylic acid from acrolein should always result in a lower value of the oxygen activity when applied in a mixture containing acrolein than in a mixture containing the same amount of acrylic acid, thus indicating a high stability of the desired partially oxidized product acrylic acid (${}^K\lambda_{\text{Acrylic Acid}} \gg 1$). Low stability of the metastable intermediate is the main reason for the very poor yields of partially oxidized products in the case of low (C1–C3) alkane oxidation (22). However, SEP cannot help to answer the question whether the grain selectivity with respect to acrylic acid ${}^K S_{\text{acrylic acid}}$ shows reasonably high values, for SEP cannot make a difference between selective oxygen (leading to the production of acrylic acid) and unselective oxygen (leading to the formation of by-products). Moreover, the oxygen activity is correlated to the total rate of oxygen consumption on the catalyst.

If different phases composing a multicomponent catalyst are identified and can be synthesized separately, it is promising to determine the oxygen activity profiles in those single phases as well as the profile in the multicomponent catalyst itself, resulting from the evolution of the same gas phase.

We can expect that the combination of the kinetic and potentiometric measurements will give a strong hint concerning the role of the different phases within the reaction network and may lead to practical correlations between the oxidation state of a catalyst and its kinetic behavior (selectivity and activity) during oxidation. This approach has been exemplified recently (10).

ACKNOWLEDGMENT

The present work has been sponsored by the Ministry of Research and Technology of the German Federal Republic through contract 03 D 0006.

REFERENCES

1. Recknagel, R., and Riekert, L., *Chem. Technik*. **46**, 324 (1994).
2. Haber, J., *Stud. Surf. Sci. Catal.* **72**, 279 (1992).
3. Millet, J. M. M., Pouceblanc, H., Goudurier, G., Herrmann, J. M., and Vedrine, J. C., *J. Catal.* **142**, 381 (1993).
4. Delmon, B., and Weng, L. T., *Appl. Catal. A* **81**, 141 (1992).
5. Legendre, O., Jäger, Ph., and Brunelle, J. P., *Stud. Surf. Sci. Catal.* **72**, 387 (1992).
6. Wagner, C., *Adv. Catal.* **21**, 323 (1970).
7. Recknagel, R., Thesis, Karlsruhe (TH), 1994.
8. Lintz, H.-G., and Vayenas, C., *Angew. Chem. Int. Ed. Engl.* **28**, 708 (1989).
9. Hildenbrand, H.-H., and Lintz, H.-G., *Ber. Bunsen-Ges. Phys. Chem.* **95**, 1191 (1991).
10. Estenfelder, M., and Lintz, H.-G., *Appl. Catal. A* **202**, 223 (2000).
11. Brück, J., Lintz, H.-G., and Valentin, G., *Solid State Ionics* **112**, 10 (1998).
12. Krabetz, R., Ferrmann, W., Engelbach, H., Palm, P., Sommer, K., and Spahn, H., EP17000 (1980).
13. Breiter, S., and Lintz, H.-G., *Chem. Eng. Sci.* **50**, 785 (1995).
14. Riekert, L., *Appl. Catal.* **15**, 89 (1985).
15. Estenfelder, M., Lintz, H.-G., Stein, B., and Gaube, J., *Chem. Eng. Process.* **37**, 109 (1998).
16. Estenfelder, M., and Lintz, H.-G., *Catal. Lett.* **57**, 71 (1999).
17. Wagner, C., and Hauffe, K., *Ztschr. Elektrochem.* **44**, 172 (1938).
18. Mars, P., and van Krevelen, D. W., *Spec. Suppl. Chem. Eng. Sci.* **3**, 41 (1954).
19. Brück, J., Thesis, Karlsruhe (TH) (1995).
20. Wagner, C., *Ber. Bunsen-Ges. Phys. Chem.* **74**, 401 (1970).
21. Hildenbrand, H. H., and Lintz, H.-G., *Appl. Catal.* **65**, 241 (1990).
22. Cavani, F., and Trifiro, F., *Stud. Surf. Sci. Catal.* **110**, 19 (1997).